nature chemistry

Article

https://doi.org/10.1038/s41557-025-01970-1

Copper-catalysed asymmetric cross-coupling reactions tolerant of highly reactive radicals

Received: 21 September 2024

Accepted: 9 September 2025

Published online: 20 October 2025

Check for updates

Li-Wen Fan[1,2,4], Jun-Bin Tang[1,4], Li-Lei Wang[1,4], Zeng Gao[1,4], Ji-Ren Liu[1,3,4], Yu-Shuai Zhang[1,2], Dai-Lei Yuan[1,2], Li Qin[1], Yu Tian[1], Zhi-Chao Chen[1], Fu Liu[1], Jin-Min Xiang[1], Pei-Jie Huang[1], Wei-Long Liu[1], Chen-Yu Xiao[1,2], Cheng Luan[1,2], Zhong-Liang Li[1], Xin Hong[3] ✉, Zhe Dong[1] ✉, Qiang-Shuai Gu[1,2] ✉ & Xin-Yuan Liu[1] ✉

Achieving high enantioselectivity in asymmetric catalysis, especially with very reactive species such as radicals, often comes at the expense of generality. Radicals with exceptionally high reactivity are typically unsuitable for existing asymmetric methodologies. Here we present a general catalytic approach to asymmetric radical cross-coupling that combines copper-catalysed enantioselective stereocentre resolution or formation with copper-mediated, chirality-transferring radical substitution. This sequential strategy enables the efficient coupling of over 50 distinct carbon-, nitrogen-, oxygen-, sulfur- and phosphorus-centred radicals, including highly reactive methyl, *tert*-butoxyl and phenyl radicals, yielding structurally diverse C-, P- and S-chiral compounds with outstanding enantioselectivity. Our method thus provides a unified platform for the synthesis of carbon, phosphorus and sulfur stereocentres, with important implications for the preparation of chiral molecules relevant to medicinal chemistry and related disciplines. Furthermore, this sequential stereodiscrimination and chirality transfer strategy offers a promising blueprint for the development of highly enantioselective methodologies applicable to other classes of highly reactive species beyond radicals.

Robust methods in organic synthesis are fundamental to the creation of new molecules, enabling advances across chemistry and related disciplines[1,2]. A central goal in synthetic chemistry is the development of reactions that combine high yields with broad substrate scope, thereby maximizing reaction generality[3]. Achieving this level of generality in catalytic asymmetric reactions is particularly challenging, as optimizing for both selectivity and yield often involves addressing the complex issue of enantioselectivity[4,5]. The challenge is especially pronounced for very reactive species, such as radicals, where the control of stereochemistry remains formidable[6,7].

Traditional approaches to catalytic asymmetric radical bond-forming processes[6,7], including coupling, addition and substitution, typically rely on stereodiscrimination between a prochiral radical or its reaction partner and the catalyst (see Fig. 1a and Supplementary Fig. 1 for discussions on 'free' and catalyst-bound radicals, respectively). However, the activation barriers for these processes are generally low, which makes it challenging to achieve sufficient energy differences between competing diastereomeric transition states. As a result, catalytic reactions involving highly unstable and reactive radicals often afford poor or only marginal enantioselectivity[7] (Fig. 1b). Although

[1]Shenzhen Grubbs Institute, Department of Chemistry, and Guangming Advanced Research Institute, Southern University of Science and Technology, Shenzhen, China. [2]Shenzhen Key Laboratory of Small Molecule Drug Discovery and Synthesis, Southern University of Science and Technology, Shenzhen, China. [3]Center of Chemistry for Frontier Technologies, Department of Chemistry, State Key Laboratory of Clean Energy Utilization, Zhejiang University, Hangzhou, China. [4]These authors contributed equally: Li-Wen Fan, Jun-Bin Tang, Li-Lei Wang, Zeng Gao, Ji-Ren Liu.
✉e-mail: hxchem@zju.edu.cn; dongz@sustech.edu.cn; guqs@sustech.edu.cn; liuxy3@sustech.edu.cn

https://doi.org/10.1038/s41557-025-01970-1

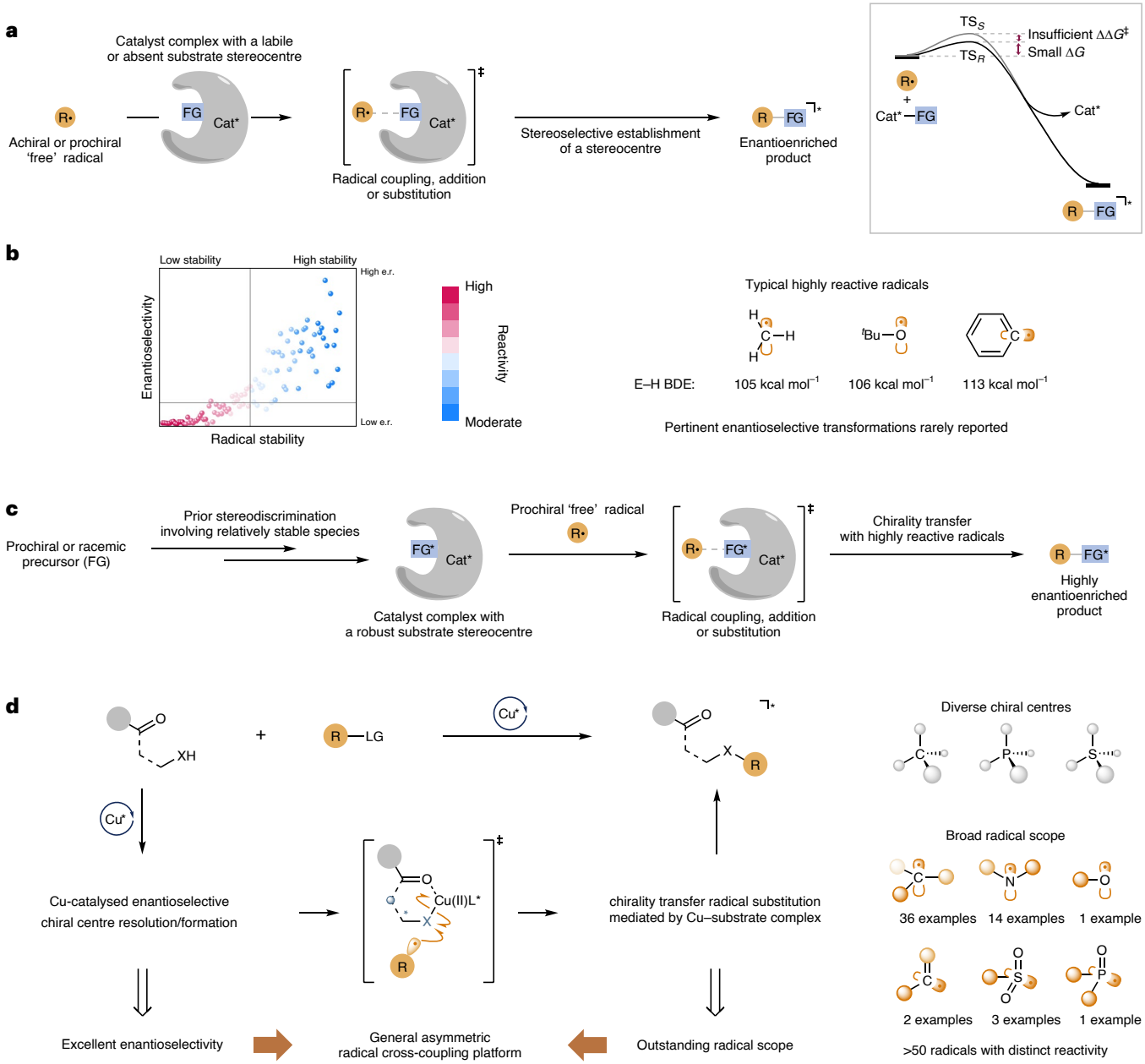

Fig. 1 | Sequential stereodiscrimination and chirality transfer strategy for asymmetric transformations of highly reactive radicals. a, Stereocontrol in elementary radical bond-forming reactions is challenging due to the high reactivity of radicals. **b**, Existing asymmetric methodologies generally fail to deliver satisfactory enantioselectivity with highly unstable radicals. Within the plotting area, a horizontal reference line at e.r. = 10:1 (90% e.e.) marks the 'good' enantioselectivity threshold, and a vertical reference line indicates the conceptual boundary between lower and higher radical stability. **c**, The proposed sequential stereodiscrimination and chirality transfer strategy addresses this by establishing stereocontrol at an early stage through the formation of relatively stable intermediates, before the involvement of highly reactive radicals. **d**, This approach enables a general copper-catalysed asymmetric radical cross-coupling platform by integrating enantioselective stereocentre resolution or formation with chirality transfer mediated by a copper–substrate complex in radical substitution reactions. FG, functional group; Cat*, chiral catalyst; FG*, functional group bearing stereocenter; R·, radical; TS_R, transition state of *R* isomer; TS_S, transition state of *S* isomer; ΔG, free-energy barrier; $\Delta\Delta G^{\ddagger}$, free-energy difference between diastereomeric pathways; e.r., enantiomeric ratio; E–H, element–hydrogen bond; ᵗBu, *tert*-butyl; Cu*, chiral copper catalyst; LG, leaving group.

catalyst–radical association or complexation strategies can sometimes improve selectivity[8–10], their successful application to achieve enantiocontrol of radicals with very high intrinsic reactivity remains limited. For example, prototypical carbon-centred radicals such as methyl radicals, which lack stabilizing (hyper)conjugation effects, are less stable than the vast majority of alkyl radicals[11] and have proven exceptionally difficult to engage in highly enantioselective transformations. To the best of our knowledge, the direct enantioselective functionalization of such radicals, without resorting to radical–polar crossover strategies[12,13], remains unreported. Even more unstable species, such as *tert*-butoxyl and phenyl radicals[11], present even greater challenges for enantioselective catalysis.

To overcome the difficulties associated with stereodiscrimination in highly reactive radical systems, we envisioned a sequential stereodiscrimination and chirality transfer strategy (Fig. 1c). In this approach, a prochiral or racemic substrate first forms a catalyst-bound complex, thereby establishing a robust stereocentre in the substrate under conditions in which the relevant species are relatively stable. This process

https://doi.org/10.1038/s41557-025-01970-1

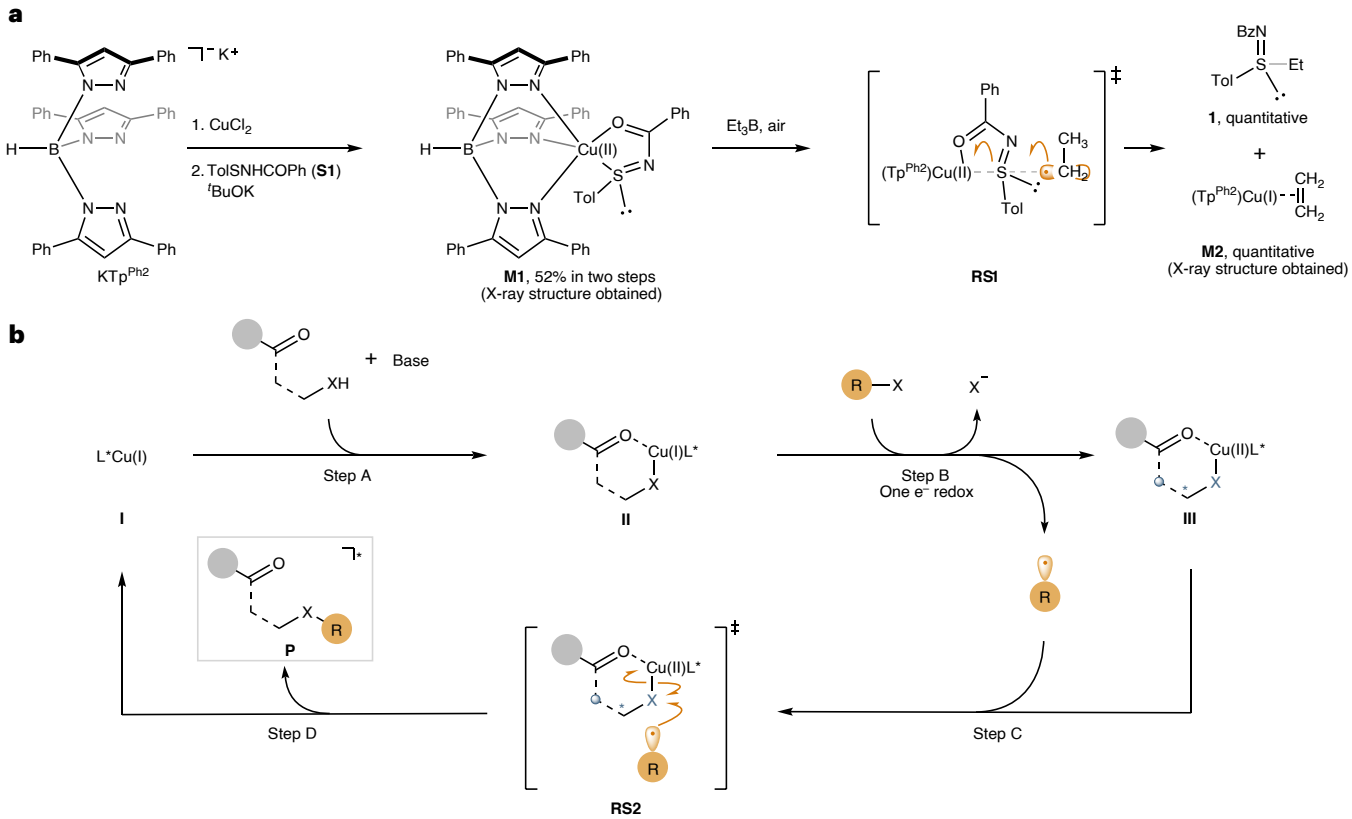

Fig. 2 | Inspirations and reaction development. a, Synthesis of the Cu(II)–sulfinimidoyl complex and subsequent radical substitution reaction with ethyl radicals. **b**, Proposed catalytic cycle for the copper-catalysed enantioselective radical cross-coupling of carbonyl-bearing substrates with electrophiles via chirality-transferring radical substitution. **c**, Copper-catalysed enantioselective O–S, P–C and S–C coupling of γ-aminocarbonyl alcohol **S2**, β-aminocarbonyl H-phosphinate **S19** and *N*-acylsulfenamide **S20** with sulfonyl, benzyl and phenyl radicals, respectively. Tp^{Ph2}, hydrotris(3,5-diphenylpyrazol-1-yl)borate; Ph, phenyl; Tol, *p*-tolyl; Et, ethyl; Bz, benzoyl; Idl, 1-indolinyl; ^{i}Pr, isopropyl; Ar, 3-fluorophenyl; e.e., enantiomeric excess; Bn, benzyl; Me, methyl; *s*, selectivity factor used to assess the kinetic resolution capability.

https://doi.org/10.1038/s41557-025-01970-1

Table 1 | Scope of the enantioselective coupling of alcohols

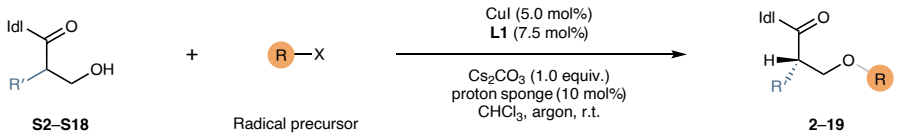

With 3-fluorophenylsulfonyl radicals

2, 47%, 92% e.e.
s = 79

3, 47%, 94% e.e.[a]
s = 100

4, 45%, 93% e.e.
s = 78

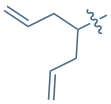

5, 47%, 91% e.e.
s = 67

6, 49%, 88% e.e.
s = 51

7, 49%, 94% e.e.
s = 121

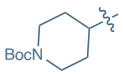

8, 50%, 93% e.e.
s = 91

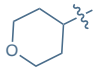

9, 50%, 91% e.e.
s = 75

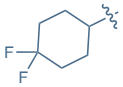

10, 48%, 91% e.e.
s = 70

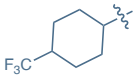

11, 40%, 92% e.e.
s = 74

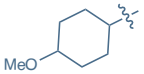

12, 48%, 94% e.e.
s = 115

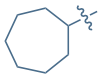

13, 49%, 92% e.e.
s = 85

With other radicals

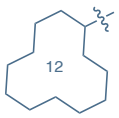

14, 43%, 95% e.e.
s = 102

15, 35%, 83% e.e.[a]

16, 35%, 87% e.e.[a]

17, 40%, 84% e.e.[a,b]

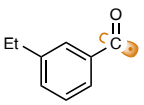

18, 33%, 90% e.e.[a,c]

19, 25%, 79% e.e.[a,d]

Standard reaction conditions: γ-aminocarbonyl alcohol (0.20 mmol, 1.0 equiv.), 3-fluorobenzenesulfonyl chloride **H1** (0.18 mmol, 0.90 equiv.), CuI (0.010 mmol, 5.0 mol%), **L1** (0.015 mmol, 7.5 mol%), Cs_2CO_3 (0.20 mmol, 1.0 equiv.) and proton sponge (0.020 mmol, 10 mol%) in $CHCl_3$ (1.0 ml) at r.t. for 48 h under argon. Isolated yields are given. The e.e. values are based on chiral HPLC analysis. Selectivity factor $s=\ln[(1-c)(1-e.e._S)]/\ln[(1-c)(1+e.e._S)]$, where conversion $c=e.e._S/(e.e._S+e.e._P)$, and $e.e._S$ and $e.e._P$ are the enantiomeric excesses of the recovered substrate and the obtained product, respectively. When R is 3-fluorophenylsulfonyl, R′ refers to the various substituents presented in Table 1. [a]See Supplementary Section 6 for details of modified conditions. [b]With 2-bromobenzenesulfonyl chloride **H2** as sulfonyl radical precursor. [c]With 3-ethylbenzaldehyde **C1** and *tert*-butyl propyl carbonoperoxoate **O2** as acyl radical precursors. [d]With diethyl ({[(2,6-dichlorobenzoyl)oxy]imino}(*p*-tolyl)methyl)phosphonate **P1** as phosphonyl radical precursor. r.t., room temperature; nBu, *n*-butyl; Boc, *tert*-butyloxycarbonyl.

facilitates stereocontrol at an early stage, before the engagement of highly reactive radicals. Subsequently, the catalyst-bound intermediate undergoes a radical reaction with high stereochemical fidelity, which may proceed with either retention or inversion of the established stereocentre, resulting in overall excellent chirality transfer. Notably, as the steps leading to the catalyst complex typically involve higher activation barriers than the subsequent rapid reactions with highly reactive radicals, achieving a sufficiently high stereoselectivity for a specific diastereomer during complex formation becomes more feasible. This selectivity ensures that only the desired stereoisomer participates in the subsequent radical reaction, while undesired pathways are effectively suppressed. Thus, this strategy leverages the stereodiscrimination of relatively stable intermediates, rather than highly reactive radical species, to achieve efficient and selective stereocontrol in otherwise challenging radical transformations.

Motivated by the generally high reaction rates and well-defined stereochemical outcomes[14] of radical substitution reactions[15], particularly in transition metal catalysis[8,16,17], we identified radical substitution as a promising platform for chirality transfer. Radical substitution processes are already widely employed to construct diverse carbon–carbon[18–22], carbon–heteroatom[17,23–28] and heteroatom–heteroatom[29] bonds. However, the development of highly enantioselective radical substitution reactions[19–28] that accommodate a broad range of radical species, including highly reactive ones, remains an unmet challenge.

Here we report the development of a highly versatile and general catalytic asymmetric radical cross-coupling of γ-aminocarbonyl alcohols, β-aminocarbonyl H-phosphinates and *N*-acylsulfenamides with a diverse array of electrophiles (Fig. 1d). This method accommodates over 50 different C-, N-, O-, S- and P-centred radicals, especially those very reactive methyl, *tert*-butoxyl and phenyl radicals, enabling access to a wide variety of enantioenriched C-, P- and S-chiral compounds. The excellent tolerance of highly reactive radicals in this reaction is achieved through a strategy that involves copper-catalysed enantioselective stereocentre formation or resolution, followed by chirality-transferring radical substitution mediated by a copper–nucleophile complex.

Results and discussion

Design plan and stoichiometric experiments

The past decade has seen rapid advances in transition metal-catalysed asymmetric radical cross-coupling reactions[30,31]. However, current methods rely heavily on enantioselective reductive elimination to forge stereocentres. To address the issue of enantioselectivity with highly reactive radicals through the sequential stereodiscrimination and chirality transfer strategy discussed above, we initially assumed that the preceding oxidative addition would likely determine the enantioselectivity (for example, Step B in Fig. 2b). The following chirality-transferring radical substitution would then deliver the enantioenriched product (for example, Step D in Fig. 2b). In this scenario, the highly stereoselective formation of a chiral L^*M^{n+1}–Nu* complex (L*, chiral ligand; M, transition metal center); for example, intermediate **III** in Fig. 2b) with a configurationally stable chiral nucleophile (Nu*) motif would be greatly preferred. With this in mind, we promptly identified sulfur nucleophiles as promising candidates given the often robust metal–S bonds[32]. In addition, S(II) and S(IV) compounds have a pronounced propensity to engage in intramolecular homolytic substitution (S_Hi) reactions[33,34], with particularly high stereochemical fidelity in some cases[35].

S(IV)–metal complexes with S-stereogenic centres can be formed through S(II)–S(IV) tautomerization in bivalent sulfur compounds, such as *N*-acylsulfenamides[36], upon deprotonation. Thus, we initially chose *N*-acylsulfenamides as nucleophiles and proceeded to verify

https://doi.org/10.1038/s41557-025-01970-1

Table 2 | Scope of the enantioselective coupling of H-phosphinates

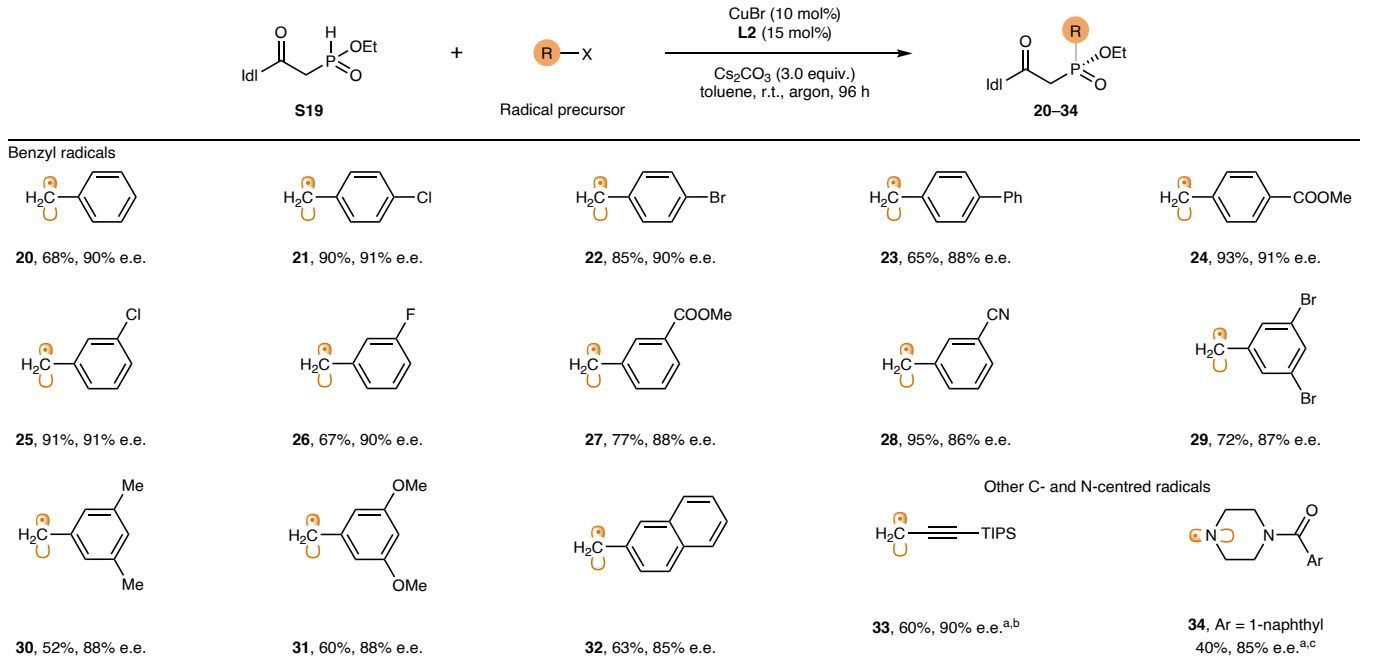

Standard reaction conditions: **S19** (0.10 mmol, 1.0 equiv.), benzyl bromide (0.15 mmol, 1.5 equiv.), CuBr (0.010 mmol, 10 mol%), **L2** (0.015 mmol, 15 mol%) and Cs_2CO_3 (0.30 mmol, 3.0 equiv.) in toluene (4.0 ml) at r.t. for 4 d under argon. Isolated yields are given. The e.e. values are based on chiral HPLC analysis. [a]See Supplementary Section 6 for details of modified conditions. [b]With 3-triisopropylsilylpropargyl bromide **C15** as propargyl radical precursor. [c]With 1-benzoyloxy-4-(1-naphthoyl)piperazine **N1** as aminyl radical precursor. TIPS, triisopropylsilyl.

the above-mentioned hypothesis using several stoichiometric control experiments. Following our recent achievements in copper-catalysed asymmetric radical carbon–heteroatom bond formation[27,37], we reasoned that copper would be the ideal transition metal catalyst due to its high resistance to sulfur poisoning. When *N*-acylsulfenamide **S1** was mixed with copper in the presence of base, a well-defined copper(II)–sulfinimidoyl complex **M1** was formed instead of a copper(II)–amido complex (Fig. 2a; see Supplementary Fig. 2 for the X-ray structure of **M1**). More encouragingly, ethylation of the S(IV) centre occurred quantitatively when **M1** was treated with triethylborane under standard conditions for ethyl radical generation. In addition to the sulfilimine product **1**, the ethylene-bonded copper(I) complex **M2**[38] was also isolated in quantitative yield and fully characterized by X-ray diffraction analysis (Fig. 2a; see Supplementary Fig. 3 for the X-ray structure of **M2**). We strongly believe that this ethylation reaction is a standard radical substitution process that occurs at the S(IV) centre as the copper centre is largely coordinatively saturated. The resulting product-bound copper(I) complex likely undergoes ligand exchange with the ethylene generated in situ[39], thereby affording **M2** and releasing **1**, as detailed in the proposed mechanism shown in Supplementary Fig. 10. These findings suggested that copper(I) species are a viable 'radical leaving group' for advancing radical substitution-based asymmetric catalysis (for example, Step D in Fig. 2b). Unfortunately, all attempts to isolate the optically active complex **M1** failed at this stage. To probe the likelihood of a chirality-transferring radical substitution, we investigated the intramolecular radical substitution reaction of an enantioenriched sulfilimine as a model (Supplementary Fig. 11). When treated with supersilane (tris(trimethylsilyl)silane) and triethylborane under ambient conditions, the chiral S(IV) centre underwent radical substitution with 100% inversion, demonstrating high chirality-transferring fidelity. Overall, these experiments provided favourable evidence for the feasibility of a catalytic cycle involving an enantiodetermining oxidative addition followed by chirality-transferring radical substitution (Fig. 2b).

Reaction development and scope

The encouraging results from the stoichiometric reactions motivated us to explore the catalytic conditions using alcohol **S2**, H-phosphinate **S19** and sulfenamide **S20** as substrates to achieve various stereocentres (Fig. 2c). The tethered carbonyl groups in these compounds were introduced as anchors to enhance the stereodiscrimination during the formation of the envisioned chiral L^*M^{n+1}–Nu* complex. Following a series of brief screening campaigns (Supplementary Tables 1, 4 and 12), we observed highly enantioselective O–S, P–C and S–C coupling of the nucleophiles with sulfonyl, benzyl and phenyl radicals, respectively, under copper catalysis with chiral multidentate anionic ligands **L1**–**L3**. Accordingly, highly enantioenriched C-chiral sulfonate ester **2**, P-chiral phosphinate **20** and S-chiral sulfilimine **38** were readily forged. Notably, phenyl radicals are extremely reactive species (C–H bond dissociation energy (BDE): 113 kcal mol^{-1}), and, to the best of our knowledge, their enantioselective functionalization has hitherto remained elusive.

After successfully solving the issue of enantioselectivity, we proceeded to evaluate the generality of these transformations (Tables 1–3). In the kinetic resolution of alcohols (Table 1), both acyclic (**2**–**5**) and cyclic (**6**–**14**) secondary alkyl groups at the β-position were well tolerated (see Supplementary Figs. 4 and 5 for the X-ray structures of enantioenriched **S5** and **9**, respectively). In addition, primary (**15**) and tertiary (**16**) alkyl groups, as well as a phenyl group (**17**), at the same position also provided notably high enantioselectivities. More importantly, in addition to sulfonyl radicals, acyl and phosphonyl radicals proved suitable for the reaction (see Supplementary Tables 2 and 3 for the optimization of conditions), delivering the desired products **18** and **19**, respectively, with excellent-to-good enantioselectivity, although at the expense of low reaction efficiency. Regarding the coupling of H-phosphinates (Table 2), a broad range of unsubstituted and substituted benzyl radicals (**20**–**32**) were also suitable for this reaction (see Supplementary Fig. 6 for the X-ray structure of **20**). In addition, propargyl and aminyl radicals also worked well (see Supplementary Tables 5 and 6 for the optimization of conditions), affording the P–C and P–N

https://doi.org/10.1038/s41557-025-01970-1

Table 3 | Scope of radicals in the enantioselective coupling with *N*-acylsulfenamides

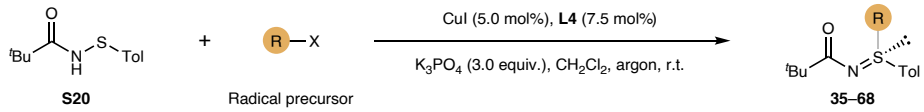

Representative C-, N- and O-centred radicals

R1 (90 kcal mol^{-1})[a] **R2** (98 kcal mol^{-1})[b] **R3** (106 kcal mol^{-1})[b] **R4** (113 kcal mol^{-1})[b] **R5** (95 kcal mol^{-1})[b] **R6** (106 kcal mol^{-1})[b]

RS

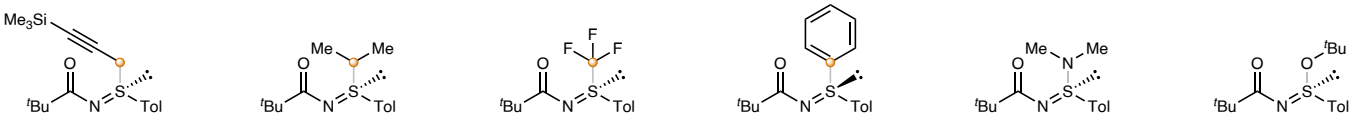

35, 95%, 98% e.e. **36**, 85%, 93% e.e.[c,d] **37**, 95%, 97% e.e.[c,e] **38**, 54%, 95% e.e.[c,f] **39**, 75%, 95% e.e.[c,g] **40**, 50%, 99% e.e.[c,h]

Other C-centred radicals

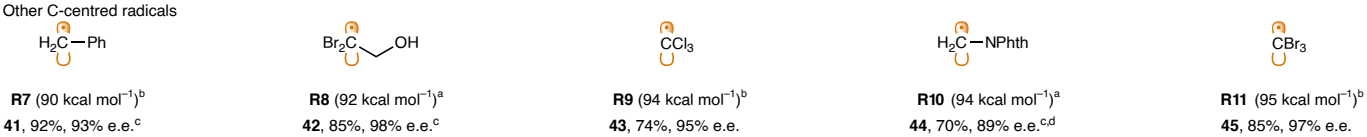

R7 (90 kcal mol^{-1})[b] **R8** (92 kcal mol^{-1})[a] **R9** (94 kcal mol^{-1})[b] **R10** (94 kcal mol^{-1})[a] **R11** (95 kcal mol^{-1})[b]

41, 92%, 93% e.e.[c] **42**, 85%, 98% e.e.[c] **43**, 74%, 95% e.e. **44**, 70%, 89% e.e.[c,d] **45**, 85%, 97% e.e.

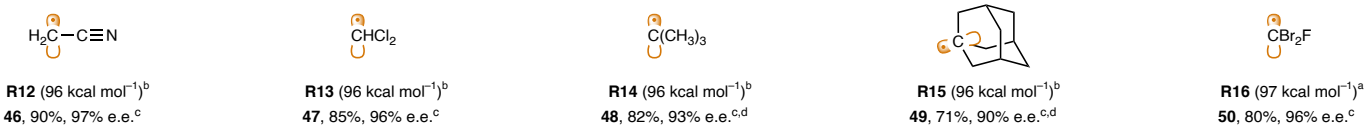

R12 (96 kcal mol^{-1})[b] **R13** (96 kcal mol^{-1})[b] **R14** (96 kcal mol^{-1})[b] **R15** (96 kcal mol^{-1})[b] **R16** (97 kcal mol^{-1})[a]

46, 90%, 97% e.e.[c] **47**, 85%, 96% e.e.[c] **48**, 82%, 93% e.e.[c,d] **49**, 71%, 90% e.e.[c,d] **50**, 80%, 96% e.e.[c]

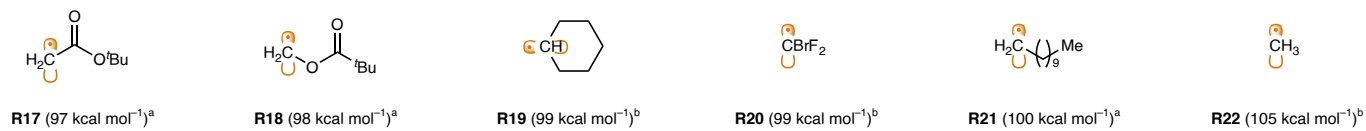

R17 (97 kcal mol^{-1})[a] **R18** (98 kcal mol^{-1})[a] **R19** (99 kcal mol^{-1})[b] **R20** (99 kcal mol^{-1})[b] **R21** (100 kcal mol^{-1})[a] **R22** (105 kcal mol^{-1})[b]

51, 95%, 93% e.e.[c,d] **52**, 92%, 91% e.e.[c,d] **53**, 95%, 92% e.e.[c,d] **54**, 71%, 96% e.e.[c] **55**, 72%, 92% e.e.[c,d] **56**, 72%, 91% e.e.[c,d]

Other N-centred radicals[g]

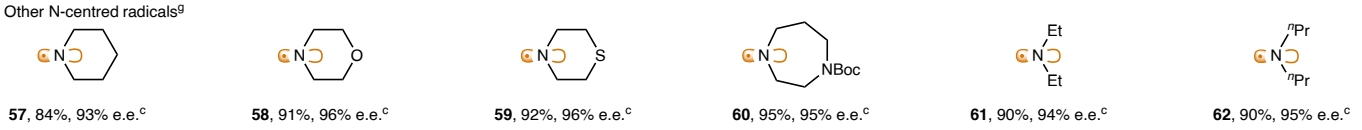

57, 84%, 93% e.e.[c] **58**, 91%, 96% e.e.[c] **59**, 92%, 96% e.e.[c] **60**, 95%, 95% e.e.[c] **61**, 90%, 94% e.e.[c] **62**, 90%, 95% e.e.[c]

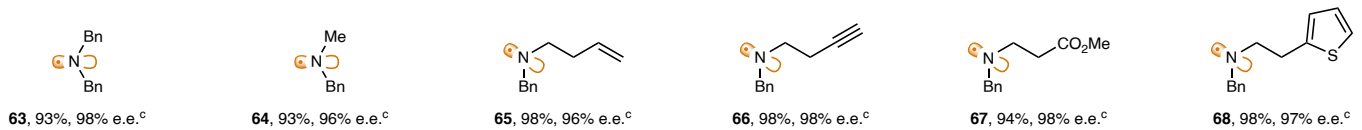

63, 93%, 98% e.e.[c] **64**, 93%, 96% e.e.[c] **65**, 98%, 96% e.e.[c] **66**, 98%, 98% e.e.[c] **67**, 94%, 98% e.e.[c] **68**, 98%, 97% e.e.[c]

Standard reaction conditions: *N*-acylsulfenamide **S20** (0.20 mmol), alkyl bromide (1.2 equiv.), CuI (5.0 mol%), **L4** (7.5 mol%) and K_3PO_4 (3.0 equiv.) in CH_2Cl_2 (2.0 ml) at r.t. under argon. Isolated yields are given. The e.e. values are based on chiral HPLC analysis. [a]Predicted C–H BDE by DeepSynthesis at http://pka.luoszgroup.com/bde_prediction. [b]Experimental C–H BDE from ref. 41. [c]See Supplementary Section 6 for details of modified conditions. [d]With alkyl iodide and $MesN_2BF_4$ as alkyl radical precursors. [e]With Togni's reagent II as trifluoromethyl radical precursor. [f]With PhN_2BF_4 as phenyl radical precursor. [g]With *N*-benzoyloxyamine as aminyl radical precursor. [h]With ^{t}BuOOH as *tert*-butoxyl radical precursor. In addition to **40**, (S_S)-TolS(=O)NHPiv **40′** (40% yield, 91% e.e.) was also formed. Modifying the work-up procedure led to only **40′** in 95% yield with 96% e.e. (see Supplementary Fig. 12 for details). RS, radical substitution; Phth, phthaloyl; ^{n}Pr, *n*-propyl; Mes, mesityl; Piv, *tert*-butylcarbonyl.

coupling products **33** and **34**, respectively, with high enantioselectivity. It is worth mentioning that this method enables the direct conversion of racemic phosphinates into chiral phosphonamidates, which are now considered privileged structures in nucleoside drug discovery.

To further demonstrate the radical generality of this strategy, we next investigated the scope of electrophiles using *N*-acylsulfenamide **S20** as the standard nucleophile (Table 3). We examined a range of alkyl halides as precursors to alkyl radicals, which were generated using copper-catalysed direct halogen atom transfer (XAT) or indirect aryl radical-mediated XAT processes[40]. The copper-catalysed strategy effectively produced a diverse array of chiral sulfilimines (**35**–**37** and **41**–**56**) from various alkyl radicals (see Supplementary Figs. 7 and 8 for the X-ray structures of **36** and **46**, respectively, and Supplementary Tables 7–11 for the optimization of conditions). These alkyl radicals exhibited varying stability[11,41], ranging from the highly stabilized benzyl radical **R7** (C–H BDE: 90 kcal mol^{-1}) to the very unstable methyl radical **R22** (C–H BDE: 105 kcal mol^{-1}), and all gave excellent enantioselectivities and high isolated yields. In addition to radical stability, the present asymmetric cross-coupling reaction showed substantial insensitivity towards radical steric properties,

https://doi.org/10.1038/s41557-025-01970-1

Table 4 | Scope of *N*-acylsulfenamides

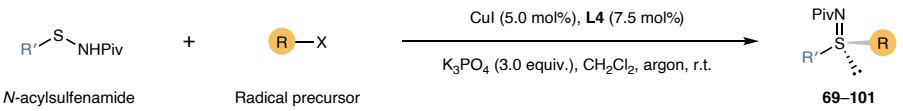

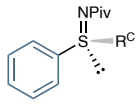
69, 94%, 98% e.e.

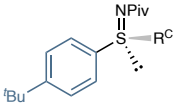
70, 97%, 95% e.e.

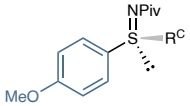
71, 80%, 96% e.e.

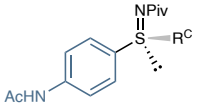
72, 80%, 99% e.e.

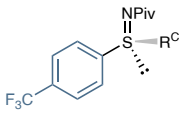
73, 96%, 90% e.e.

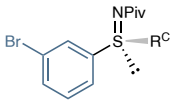
74, 90%, 92% e.e.

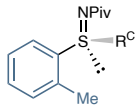
75, 78%, 95% e.e.

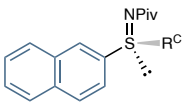
76, 81%, 98% e.e.

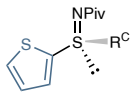
77, 80%, 93% e.e.

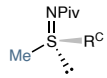
78, 90%, 81% e.e.[a]

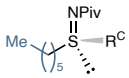
79, 78%, 96% e.e.

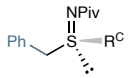
80, 75%, 94% e.e.

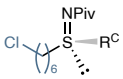
81, 90%, 96% e.e.[a]

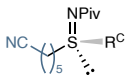
82, 74%, 94% e.e.[a]

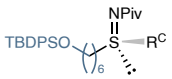
83, 74%, 94% e.e.[a]

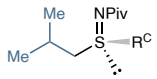
84, 84%, 96% e.e.

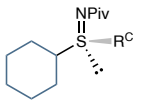
85, 80%, 98% e.e.

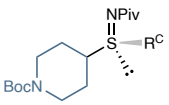
86, 83%, 94% e.e.

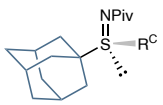
87, 54%, 89% e.e.

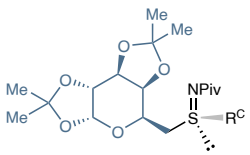
88, 96%, >20:1 d.r.

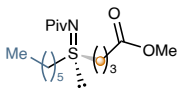
89, 75%, 96% e.e.[a,b]

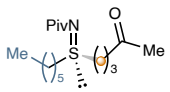
90, 77%, 96% e.e.[a,b]

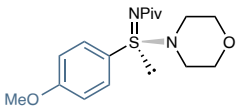
91, 95%, 96% e.e.[a,c]

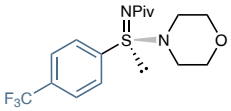
92, 67%, 96% e.e.[a,c]

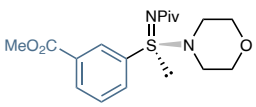
93, 86%, 96% e.e.[a,c]

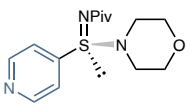
94, 75%, 97% e.e.[a,c]

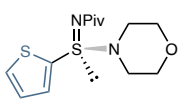
95, 73%, 95% e.e.[a,c]

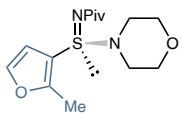
96, 44%, 97% e.e.[a,c]

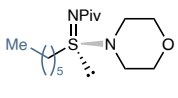
97, 95%, 97% e.e.[a,c]

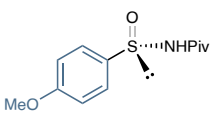
98, 98%, 94% e.e.[a,d]

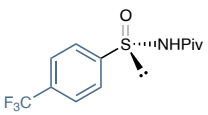
99, 98%, 92% e.e.[a,d]

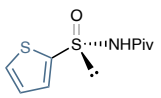
100, 95%, 93% e.e.[a,d]

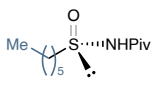
101, 82%, 91% e.e.[a,d]

Standard reaction conditions: *N*-acylsulfenamide (0.20 mmol), radical precursor (1.2 equiv.), CuI (5.0 mol%), **L4** (7.5 mol%) and K_3PO_4 (3.0 equiv.) in CH_2Cl_2 (2.0 ml) at r.t. under argon. Isolated yields are given. The e.e. values are based on chiral HPLC analysis. [a]See Supplementary Section 6 for details of modified conditions. [b]With alkyl iodide and $MesN_2BF_4$ as alkyl radical precursors. [c]With *N*-benzoyloxymorpholine. [d]With ^{t}BuOOH. R^C, $CH_2C{\equiv}CSiMe_3$; Ac, acetyl; TBDPS, *tert*-butyldiphenylsilyl; d.r., diastereomeric ratio.

as evidenced by the fact that monosubstituted (for example, **R1**, **R7**, **R10** and **R17**), disubstituted (**R2**, **R13** and **R19**) and trisubstituted (for example, **R11**, **R14** and **R15**) alkyl radicals all afforded good yields and excellent enantioselectivities (≥89% e.e.). Perhaps most remarkably, the enantioselectivity was not affected by radical polarity[42,43]. Both nucleophilic (for example, **R10** and **R14**) and electrophilic (for example, **R9** and **R12**) alkyl radicals exhibited comparably high enantioselectivity. More importantly, both the nucleophilic dimethylaminyl radical **R5** and the highly electrophilic *tert*-butoxyl radical **R6** readily underwent the coupling reaction (see Supplementary Tables 13 and 14 for the optimization of conditions), yielding chiral sulfinamidine **39** and sulfinimidate ester **40** with high e.e. It is worth mentioning that the *tert*-butoxyl radical **R6** is known to undergo rapid β-scission (rate constant k_β at 295 K in acetonitrile: $6 \times 10^4\ s^{-1}$)[44], resulting in methyl radicals and acetone. However, in our reaction, the coupling product **40** was efficiently formed while acetone was barely detected, indicating a very fast radical substitution process, as originally presumed. Interestingly, we were able to convert *N*-acylsulfenamide **S20** into a range of chiral sulfinamidines **57**–**68** (see Supplementary Fig. 9 for the X-ray structure of **57**) using highly diverse aminyl radicals derived from their corresponding *N*-benzoyloxyamine precursors. Overall, we believe that the present transformation has unprecedented radical scope in the field of catalytic asymmetric radical cross-coupling reactions.

It is noteworthy that chiral S(IV) and S(VI) centres are not only important chiral synthons in asymmetric organic synthesis but also prevalent functional groups in medicinal chemistry (Supplementary Fig. 13)[45,46]. Some elegant catalytic asymmetric methods have been disclosed for the synthesis of these valuable molecules[47–51] (see Supplementary Fig. 14 for further discussions). However, a comprehensive approach to attain assorted S(IV) and S(VI) centres with a broad spectrum of substitutions remains to be devised. Accordingly, we next sought to evaluate the scope of the *N*-acylsulfenamide coupling partner. As shown in Table 4, multiple *N*-acylsulfenamides containing *S*-(hetero)aryl and *S*-alkyl groups produced the desired sulfilimine products **69**–**90** in good yields with excellent enantioselectivities. Notably, neither their steric properties (**85**–**87**) nor pre-existing stereocentres (**88**) impacted the efficiency or enantioselectivity of the reaction. Our protocols were also effective in accessing the chiral

https://doi.org/10.1038/s41557-025-01970-1

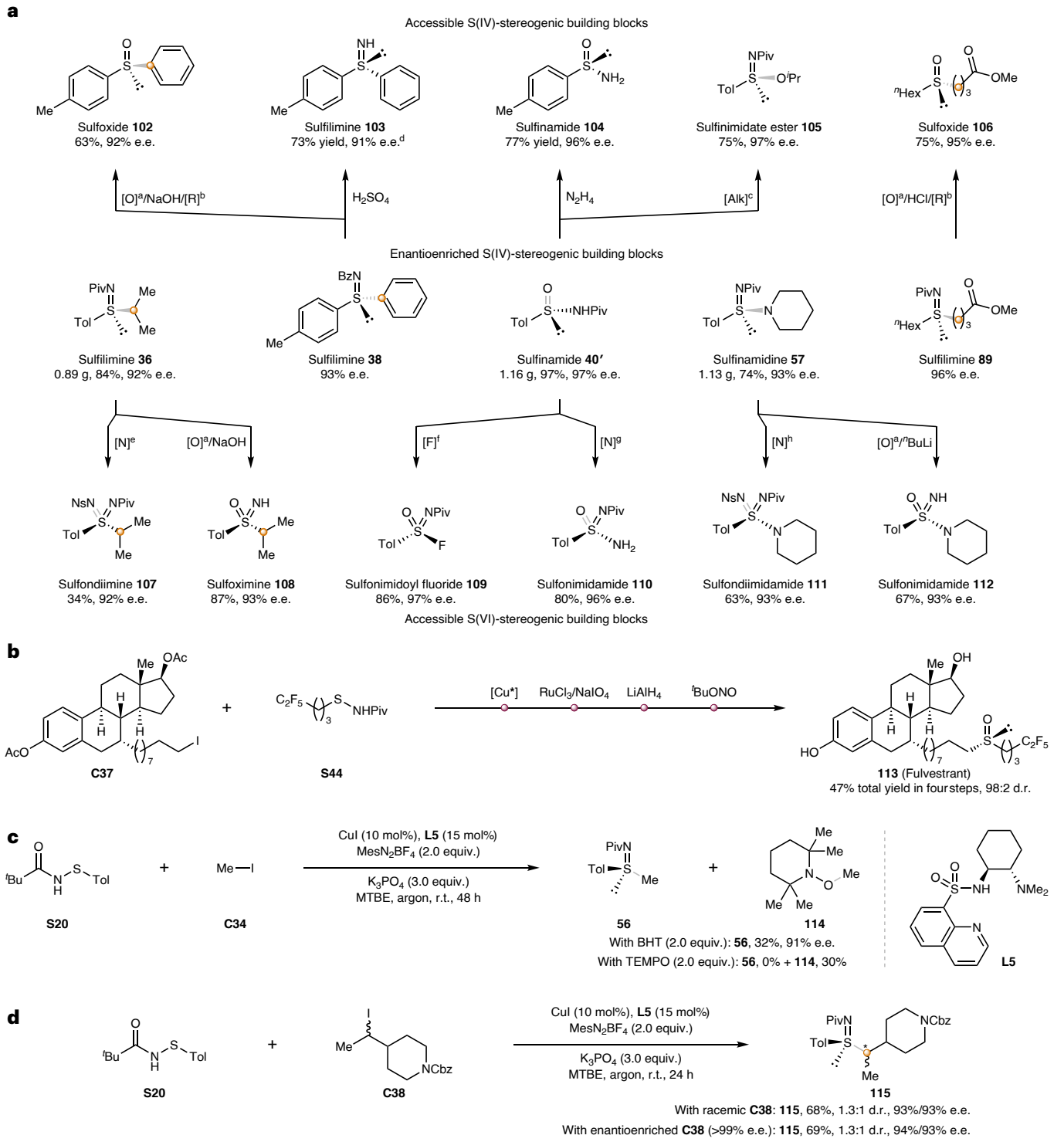

Fig. 3 | Synthetic utility and mechanistic studies. a, Transformations of enantioenriched S-chiral products. **b**, Enantioselective synthesis of fulvestrant. **c**, Control experiments with the radical traps BHT and TEMPO markedly inhibited the reaction and led to the formation of radical-trapped product **114. d**, Control experiments using an enantioenriched and racemic secondary alkyl iodide gave identical diastereoselectivity, supporting a radical mechanism. [a]$RuCl_3$ and $NaIO_4$. [b]^{t}BuONO. [c]PrI and K_2CO_3. [d]From **38**, obtained with 94% e.e. The e.e. value was determined after reacylation. [e]AgNTf, ^{t}Bu$_3$tpy and PhI=NNs. [f]NaH, Selectfluor and KOAc. [g]NH_3(aq) and ^{t}BuOCl. [h]AgNTf, ^{t}Bu$_3$tpy, PhI=NNs and $NaHCO_3$. [O], oxidation; [R], reduction; [Alk], alkylation; [n]Hex, *n*-hexyl; [N], imidation or amination; [F], fluorination; Ns, *p*-nitrobenzenesulfonyl; MTBE, methyl *tert*-butyl ether; Tf, trifluoromethanesulfonyl; ^{t}Bu$_3$tpy, 4,4′,4″-tri-*tert*-butyl-2,2′:6′,2″-terpyridine; Cbz, benzyloxycarbonyl.

sulfinamidines **91**–**97** and sulfinamides **98**–**101**[52] with different nitrogen and oxygen electrophiles. More importantly, many medicinally important functional groups were well tolerated, such as acetanilide (**72**), primary alkyl chloride (**81**), protected galactopyranose (**88**), pyridine (**94**), furan (**96**) and thiophene (**77**, **95** and **100**).

Synthetic utility

The method reported above represents a versatile coupling approach for converting *N*-acylsulfenamides into a range of chiral S(IV) centres, encompassing *N*-acylsulfilimines, *N*-acylsulfinamidines, *N*-acylsulfinamides and *tert*-butyl sulfinimidate esters. Further

manipulation of these products readily afforded deacylated sulfilimine (**103**) and sulfinamide (**104**), as well as isopropyl sulfinimidate ester (**105**; Fig. 3a, top). In addition, sulfilimines **38** and **89** could be straightforwardly transformed into sulfoxides **102** and **106** (Fig. 3a, top), respectively, which bear similar S substituents that are otherwise challenging to differentiate stereochemically by direct oxidation methods (Supplementary Fig. 14). The presence of organometallic-labile functional groups, such as carboxylic esters, also complicates the traditional stochiometric nucleophilic substitution method used to prepare S-chiral dialkylsulfoxides. Importantly, this synthetic strategy enables the rare catalytic stereoselective synthesis of a prominent anti-cancer drug (**113**; Fig. 3b), fulvestrant, which has hitherto been commercialized in its diastereomeric mixture form due to the aforementioned synthetic challenges.

An intriguing prospect involves using stereoselective reactions to convert these chiral S(IV) centres into their corresponding chiral S(VI) centres (Fig. 3a, bottom). As such, chiral sulfilimine **36** was successfully transformed into sulfondiimine **107** and sulfoximine **108**, and sulfinamidine **57** into sulfondiimidamide **111** and sulfonimidamide **112** by treatment with appropriate oxidants under catalytic conditions[46]. Furthermore, sulfinamide **40′** was oxidized to generate sulfonimidoyl fluoride **109** and sulfonimidamide **110**. Both **105**[53] and **109**[54] are well-known synthetic hubs towards a number of chiral S(IV) and S(VI) compounds. Notably, all of these reactions transferred the chiral information of the S(IV) centres quantitatively to the S(VI) centres of the products. Thus, this asymmetric radical coupling reaction offers medicinal chemists a comprehensive synthetic solution to investigate the novel chiral chemical space relating to sulfur-based bioactive molecules.

Mechanistic studies

Control experiments with radical inhibitors (2,2,6,6-tetramethylpiperidin-1-yl)oxyl (TEMPO) or 2,6-di-*tert*-butyl-4-methylphenol (BHT) led to substantial retardation of the coupling reactions with C-, N-, O-, S- and P-based electrophiles (Fig. 3c and Supplementary Figs. 15–20), supporting the presumed involvement of radical species. More intriguingly, the catalytic system could convert radicals **R7** and **R12**, generated by hydrogen atom abstraction from the corresponding hydrocarbon solvents (Supplementary Fig. 21), into the desired coupling products **41** and **46**, respectively, with high enantioselectivity, albeit in low yields. These results further confirmed the intermediacy of radical species in the coupling reactions. To rule out a nucleophilic substitution pathway, both enantioenriched and racemic alkyl iodide **C38** were subjected to the coupling reaction (Fig. 3d). The resulting product **115** displayed identical diastereoselectivity originating from the carbon stereocentres (see Supplementary Fig. 22 for details), in accord with the proposed radical mechanism rather than an ionic one. In addition, control experiments in the absence of catalyst or base failed to afford the enantioenriched products (Supplementary Tables 15 and 16), indicating that both reaction components are indispensable for this transformation. Further experiments in the presence of scalemic ligands revealed a linear relationship between the enantiopurities of the ligands and their corresponding products (Supplementary Fig. 23), supporting a 1:1 ligand/copper ratio in the enantiodetermining step. More importantly, our initial stoichiometric experiments clearly demonstrated the ready formation of Cu(II)–sulfinimidoyl complexes and their susceptibility towards radical substitution reactions (Fig. 2a). Our preliminary density functional theory studies (Supplementary Figs. 24–32 and Supplementary Tables 17–22) on the final radical bond formation step revealed a stereoinvertive S_H2-type radical substitution[15] mechanism. All these mechanistic results are in full agreement with the proposed catalytic cycle shown in Fig. 2b.

Conclusions

We have developed a highly enantioselective radical cross-coupling reaction with broad substrate scope using copper(I) catalysts in combination with chiral multidentate anionic ligands. This method efficiently achieves the enantioselective construction of C-, P- and S-centred chiral centres, demonstrating broad compatibility with a wide range of organic radicals. The remarkable tolerance towards highly reactive radicals is attributed to a sequential stereodiscrimination and chirality transfer strategy. We anticipate that this asymmetric radical coupling approach will be broadly applicable to the synthesis of both heteroatomic and carbon stereocentres, thereby advancing the field of asymmetric radical chemistry.

Online content

Any methods, additional references, Nature Portfolio reporting summaries, source data, extended data, supplementary information, acknowledgements, peer review information; details of author contributions and competing interests; and statements of data and code availability are available at https://doi.org/10.1038/s41557-025-01970-1.

References

1. Kürti, L. & Czakó, B. *Strategic Applications of Named Reactions in Organic Synthesis: Background and Detailed Mechanisms* (Elsevier, 2005).
2. Blakemore, D. C. et al. Organic synthesis provides opportunities to transform drug discovery. *Nat. Chem.* **10**, 383–394 (2018).
3. Collins, K. D. & Glorius, F. A robustness screen for the rapid assessment of chemical reactions. *Nat. Chem.* **5**, 597–601 (2013).
4. Wagen, C. C., McMinn, S. E., Kwan, E. E. & Jacobsen, E. N. Screening for generality in asymmetric catalysis. *Nature* **610**, 680–686 (2022).
5. Rein, J. et al. Generality-oriented optimization of enantioselective aminoxyl radical catalysis. *Science* **380**, 706–712 (2023).
6. Proctor, R. S. J., Colgan, A. C. & Phipps, R. J. Exploiting attractive non-covalent interactions for the enantioselective catalysis of reactions involving radical intermediates. *Nat. Chem.* **12**, 990–1004 (2020).
7. Mondal, S. et al. Enantioselective radical reactions using chiral catalysts. *Chem. Rev.* **122**, 5842–5976 (2022).
8. Lee, W.-C. C. & Zhang, X. P. Metalloradical catalysis: general approach for controlling reactivity and selectivity of homolytic radical reactions. *Angew. Chem. Int. Ed.* **63**, e202320243 (2024).
9. Li, J. et al. Site-specific allylic C–H bond functionalization with a copper-bound N-centred radical. *Nature* **574**, 516–521 (2019).
10. Zhang, H. et al. Site- and enantioselective allylic and propargylic C–H oxidation enabled by copper-based biomimetic catalysis. *Nat. Catal.* **8**, 58–66 (2025).
11. Hioe, J. & Zipse, H. in *Encyclopedia of Radicals in Chemistry, Biology and Materials* (eds Chatgilialoglu, C. & Studer, A.) https://doi.org/10.1002/9781119953678.rad012 (Wiley, 2012).
12. Li, Y. et al. Cobalt-catalysed enantioselective C(sp^3)–C(sp^3) coupling. *Nat. Catal.* **4**, 901–911 (2021).
13. Li, J. et al. Enantioselective alkylation of α-amino C(sp^3)–H bonds via photoredox and nickel catalysis. *Nat. Catal.* **7**, 889–899 (2024).
14. Upton, C. J. & Incremona, J. H. Bimolecular homolytic substitution at carbon. Stereochemical investigation. *J. Org. Chem.* **41**, 523–530 (1976).
15. Walton, J. C. Homolytic substitution: a molecular ménage à trois. *Acc. Chem. Res.* **31**, 99–107 (1998).
16. Zhang, Y., Li, K.-D. & Huang, H.-M. Bimolecular homolytic substitution (S_H2) at a transition metal. *ChemCatChem* **16**, e202400955 (2024).
17. Milan, M., Bietti, M. & Costas, M. Enantioselective aliphatic C–H bond oxidation catalyzed by bioinspired complexes. *Chem. Commun.* **54**, 9559–9570 (2018).
18. Liu, W., Lavagnino, M. N., Gould, C. A., Alcázar, J. & MacMillan, D. W. C. A biomimetic S_H2 cross-coupling mechanism for quaternary sp^3-carbon formation. *Science* **374**, 1258–1263 (2021).

19. Li, L.-J. et al. Enantioselective construction of quaternary stereocenters via cooperative photoredox/Fe/chiral primary amine triple catalysis. *J. Am. Chem. Soc.* **146**, 9404–9412 (2024).
20. Wang, Y., Wen, X., Cui, X. & Zhang, X. P. Enantioselective radical cyclization for construction of 5-membered ring structures by metalloradical C–H alkylation. *J. Am. Chem. Soc.* **140**, 4792–4796 (2018).
21. Lee, W.-C. C., Wang, D.-S., Zhu, Y. & Zhang, X. P. Iron(III)-based metalloradical catalysis for asymmetric cyclopropanation via a stepwise radical mechanism. *Nat. Chem.* **15**, 1569–1580 (2023).
22. Wang, F.-L. et al. Mechanism-based ligand design for copper-catalysed enantioconvergent C(sp^3)–C(sp) cross-coupling of tertiary electrophiles with alkynes. *Nat. Chem.* **14**, 949–957 (2022).
23. Lang, K., Torker, S., Wojtas, L. & Zhang, X. P. Asymmetric induction and enantiodivergence in catalytic radical C–H amination via enantiodifferentiative H-atom abstraction and stereoretentive radical substitution. *J. Am. Chem. Soc.* **141**, 12388–12396 (2019).
24. Lang, K., Li, C., Kim, I. & Zhang, X. P. Enantioconvergent amination of racemic tertiary C–H bonds. *J. Am. Chem. Soc.* **142**, 20902–20911 (2020).
25. Xu, P., Xie, J., Wang, D.-S. & Zhang, X. P. Metalloradical approach for concurrent control in intermolecular radical allylic C–H amination. *Nat. Chem.* **15**, 498–507 (2023).
26. Xu, H., Wang, D.-S., Zhu, Z., Deb, A. & Zhang, X. P. New mode of asymmetric induction for enantioselective radical *N*-heterobicyclization via kinetically stable chiral radical center. *Chem* **10**, 283–298 (2024).
27. Tian, Y. et al. A general copper-catalysed enantioconvergent C(sp^3)–S cross-coupling via biomimetic radical homolytic substitution. *Nat. Chem.* **16**, 466–475 (2024).
28. Zhang, Y.-F. et al. Asymmetric amination of alkyl radicals with two minimally different alkyl substituents. *Science* **388**, 283–291 (2025).
29. Cheng, Y.-F. et al. Cu-catalysed enantioselective radical heteroatomic S–O cross-coupling. *Nat. Chem.* **15**, 395–404 (2023).
30. Cherney, A. H., Kadunce, N. T. & Reisman, S. E. Enantioselective and enantiospecific transition-metal-catalyzed cross-coupling reactions of organometallic reagents to construct C–C bonds. *Chem. Rev.* **115**, 9587–9652 (2015).
31. Choi, J. & Fu, G. C. Transition metal–catalyzed alkyl-alkyl bond formation: another dimension in cross-coupling chemistry. *Science* **356**, eaaf7230 (2017).
32. Omann, L., Königs, C. D. F., Klare, H. F. T. & Oestreich, M. Cooperative catalysis at metal–sulfur bonds. *Acc. Chem. Res.* **50**, 1258–1269 (2017).
33. Crich, D. Homolytic substitution at the sulfur atom as a tool for organic synthesis. *Helv. Chim. Acta* **89**, 2167–2182 (2006).
34. Garrido-Castro, A. F., Salaverri, N., Maestro, M. C. & Alemán, J. Intramolecular homolytic substitution enabled by photoredox catalysis: sulfur, phosphorus, and silicon heterocycle synthesis from aryl halides. *Org. Lett.* **21**, 5295–5300 (2019).
35. Coulomb, J. et al. Intramolecular homolytic substitution of sulfinates and sulfinamides. *Chem. Eur. J.* **15**, 10225–10232 (2009).
36. Zhong, W. et al. Synthesis and reactivity of the imido-bridged metallothiocarboranes $CpCo(S_2C_2B_{10}H_{10})(NSO_2R)$. *Organometallics* **31**, 6658–6668 (2012).
37. Chen, J.-J. et al. Enantioconvergent Cu-catalysed *N*-alkylation of aliphatic amines. *Nature* **618**, 294–300 (2023).
38. van Dijkman, T. F. et al. Extremely bulky copper(I) complexes of $[HB(3,5\text{-}\{1\text{-naphthyl}\}_2pz)_3]^-$ and $[HB(3,5\text{-}\{2\text{-naphthyl}\}_2pz)_3]^-$ and their self-assembly on graphene. *Dalton Trans.* **46**, 6433–6446 (2017).
39. Grotewold, J., Lissi, E. A. & Scaiano, J. C. Mechanism of the autoxidation of triethylborane. Part I. Reaction in the gas phase. *J. Chem. Soc. B* https://doi.org/10.1039/J29690000475 (1969).
40. Cai, A., Yan, W., Wang, C. & Liu, W. Copper-catalyzed difluoromethylation of alkyl iodides enabled by aryl radical activation of carbon–iodine bonds. *Angew. Chem. Int. Ed.* **60**, 27070–27077 (2021).
41. Luo, Y.-R. *Comprehensive Handbook of Chemcial Bond Energies* (CRC Press, 2007).
42. Parsaee, F. et al. Radical philicity and its role in selective organic transformations. *Nat. Rev. Chem.* **5**, 486–499 (2021).
43. Garwood, J. J. A., Chen, A. D. & Nagib, D. A. Radical polarity. *J. Am. Chem. Soc.* **146**, 28034–28059 (2024).
44. Tsentalovich, Y. P., Kulik, L. V., Gritsan, N. P. & Yurkovskaya, A. V. Solvent effect on the rate of β-scission of the *tert*-butoxyl radical. *J. Phys. Chem. A* **102**, 7975–7980 (1998).
45. Zhang, Z.-X. & Willis, M. C. Sulfondiimidamides as new functional groups for synthetic and medicinal chemistry. *Chem* **8**, 1137–1146 (2022).
46. Zhang, X., Wang, F. & Tan, C.-H. Asymmetric synthesis of S(IV) and S(VI) stereogenic centers. *JACS Au* **3**, 700–714 (2023).
47. Zhang, X., Ang, E. C. X., Yang, Z., Kee, C. W. & Tan, C.-H. Synthesis of chiral sulfinate esters by asymmetric condensation. *Nature* **604**, 298–303 (2022).
48. Greenwood, N. S., Champlin, A. T. & Ellman, J. A. Catalytic enantioselective sulfur alkylation of sulfenamides for the asymmetric synthesis of sulfoximines. *J. Am. Chem. Soc.* **144**, 17808–17814 (2022).
49. van Dijk, L. et al. Data science-enabled palladium-catalyzed enantioselective aryl-carbonylation of sulfonimidamides. *J. Am. Chem. Soc.* **145**, 20959–20967 (2023).
50. Liang, Q. et al. Enantioselective Chan–Lam S-arylation of sulfenamides. *Nat. Catal.* **7**, 1010–1020 (2024).
51. Champlin, A. T., Kwon, N. Y. & Ellman, J. A. Enantioselective *S*-alkylation of sulfenamides by phase-transfer catalysis. *Angew. Chem. Int. Ed.* **63**, e202408820 (2024).
52. Robak, M. T., Herbage, M. A. & Ellman, J. A. Synthesis and applications of *tert*-butanesulfinamide. *Chem. Rev.* **110**, 3600–3740 (2010).
53. Tsuzuki, S. & Kano, T. Asymmetric synthesis of chiral sulfimides through the *O*-alkylation of enantioenriched sulfinamides and addition of carbon nucleophiles. *Angew. Chem. Int. Ed.* **62**, e202300637 (2023).
54. Homer, J. A. et al. Sulfur fluoride exchange. *Nat. Rev. Methods Primers* **3**, 58 (2023).

Methods

Representative procedure for enantioenriched C-chiral compounds

Under an argon atmosphere, an oven-dried, resealable Schlenk tube equipped with a magnetic stir bar was charged with CuI (1.9 mg, 0.010 mmol, 5.0 mol%), **L1** (9.1 mg, 0.015 mmol, 7.5 mol%), Cs_2CO_3 (65.2 mg, 0.20 mmol, 1.0 equiv.), proton sponge (4.3 mg, 0.020 mmol, 10 mol%), γ-aminocarbonyl alcohol (0.20 mmol, 1.0 equiv.) and anhydrous $CHCl_3$ (1.0 ml). The corresponding sulfonyl chloride (0.18 mmol, 0.9 equiv.) was then added and the reaction mixture was stirred at room temperature. Upon completion, the precipitate was filtered off and washed with EtOAc. It was then concentrated and the residue was purified by column chromatography on silica gel to afford the desired product.

Representative procedure for enantioenriched P-chiral compounds

An oven-dried, resealable Schlenk tube equipped with a magnetic stir bar was charged with CuBr (1.42 mg, 0.010 mmol, 10 mol%), **L2** (9.8 mg, 0.015 mmol, 15 mol%), **S19** (25.6 mg, 0.10 mmol, 1.0 equiv.), radical precursor (0.15 mmol, 1.5 equiv.) and Cs_2CO_3 (97.6 mg, 0.30 mmol, 3.0 equiv.). The tube was evacuated and backfilled with argon three times. Anhydrous toluene (4.0 ml) was then added by syringe under argon and the reaction mixture was stirred at room temperature. On completion, the precipitate was filtered off and washed with CH_2Cl_2. The filtrate was concentrated and the residue was purified by column chromatography on silica gel to afford the desired product.

Representative procedure for enantioenriched S-chiral compounds

Under an argon atmosphere, an oven-dried, resealable Schlenk tube equipped with a magnetic stir bar was charged with sulfenamide (0.20 mmol, 1.0 equiv.), CuI (1.9 mg, 0.010 mmol, 5.0 mol%), **L4** (7.9 mg, 0.015 mmol, 7.5 mol%), K_3PO_4 (127.4 mg, 0.60 mmol, 3.0 equiv.) and anhydrous CH_2Cl_2, EtOAc or MeCN (2.0 ml). The radical precursor (0.24 or 0.30 mmol, 1.2 or 1.5 equiv.) was then added and the reaction mixture was stirred at −10 to 40 °C. On completion, the precipitate was filtered off and washed with CH_2Cl_2. The filtrate was concentrated and the residue was purified by column chromatography on silica gel to afford the desired product.

Data availability

The data supporting the findings of this study are available within the paper and its Supplementary Information (experimental procedures, characterization data and DFT calculations). Crystallographic data are also available free of charge from the Cambridge Crystallographic Database Centre (CCDC) under CCDC reference numbers 2289793 (for **M1**), 2375977 (for (*R*)-**S5**), 2375978 (for **9**), 2375976 (for **20**), 2289792 (for **36**), 2289795 (for **46**) and 2289794 (for **57**). Copies of the data can be obtained free of charge via https://www.ccdc.cam.ac.uk/structures/.

Acknowledgements

We appreciate the assistance of SUSTech Core Research Facilities. We acknowledge the financial support from the National Natural Science Foundation of China (grant nos. 22025103, 92256301 and 22331006 to X.-Y.L., 22271133 to Q.-S.G., and W2512004, 22122109 and 22271253 to X.H.), the National Key R&D Program of China (grant nos. 2021YFF0701604 to X.-Y.L., 2022YFC3401104 to Z.D. and 2022YFA1504301 to X.H.), Guangdong Innovative Program (grant nos. 2019BT02Y335 to X.-Y.L. and 2021ZT09C278 to Z.D.), the Guangdong Major Project of Basic and Applied Basic Research (grant no. 2023B0303000020 to X.-Y.L. and Z.D.), Shenzhen Science and Technology Program (grant nos. KQTD20210811090112004 to X.-Y.L. and Q.-S.G., JCYJ20220818100600001 to X.-Y.L., JCYJ20220818100604009 to J.-B.T. and 20220814231741002 to Z.D.), the New Cornerstone Science Foundation through an XPLORER PRIZE (to X.-Y.L.), High-Level of Special Funds (grant no. G03050K003 to X.-Y.L.), High-Level Key Discipline Construction Project (grant no. G030210001 to X.-Y.L. and Q.-S.G.), the Starry Night Science Fund of Zhejiang University Shanghai Institute for Advanced Study (grant no. SN-ZJU-SIAS-006 to X.H.), CAS Youth Interdisciplinary Team (grant no. JCTD-2021-11 to X.H.), the Fundamental Research Funds for the Central Universities (grant nos. 226-2022-00140, 226-2022-00224, 226-2023-00115 and 226-2024-00003 to X.H), the State Key Laboratory of Clean Energy Utilization (grant no. ZJUCEU2020007 to X.H.), the State Key Laboratory of Physical Chemistry of Solid Surfaces (grant no. 202210 to X.H.), a Leading Innovation Team grant from the Department of Science and Technology of Zhejiang Province (grant no. 2022R01005 to X.H.) and the Open Research Fund of the School of Chemistry and Chemical Engineering of Henan Normal University (grant no. 2024Z01 to X.H.). Computational studies were supported by the Center for Computational Science and Engineering of Southern University of Science and Technology and the high-performance computing system at the Department of Chemistry, Zhejiang University.

Author contributions

L.-W.F., J.-B.T., L.-L.W. and Z.G. designed the experiments and analysed the data. L.-W.F., J.-B.T., L.-L.W., Z.G., Y.-S.Z., D.-L.Y., L.Q., Y.T., Z.-C.C., F.L., J.-M.X., P.-J.H., W.-L.L., C.-Y.X., C.L. and Z.-L.L. performed the experiments. J.-R.L. and X.H. designed the DFT calculations, and J.-R.L. performed the calculations. X.H., Z.D., Q.-S.G. and X.-Y.L. wrote the paper. Z.D., Q.-S.G. and X.-Y.L. conceived and supervised the project.

Competing interests

The authors declare no competing interests.

Additional information

Supplementary information The online version contains supplementary material available at https://doi.org/10.1038/s41557-025-01970-1.

Correspondence and requests for materials should be addressed to Xin Hong, Zhe Dong, Qiang-Shuai Gu or Xin-Yuan Liu.

Peer review information *Nature Chemistry* thanks the anonymous reviewers for their contribution to the peer review of this work.